Hindawi
Shock and Vibration
Volume 2019, Article ID 8348596, 18 pages
https://doi.org/10.1155/2019/8348596

Research Article

Earthquake-Induced Domino-Type Progressive Collapse in Regular, Semiregular, and Irregular Bridges

Amir Seyedkhoei,[1] **Reza Akbari**,[2] **and Shahrokh Maalek**[3]

[1]*Department of Civil Engineering, Isfahan (Khorasgan) Branch, Islamic Azad University, Isfahan, Iran*
[2]*Senior Bridge and Structural Engineer, Road Maintenance and Transportation Organization (RMTO), Tehran, Iran*
[3]*Lecturer, School of Civil Engineering, College of Engineering, University of Tehran, Tehran, Iran*

Correspondence should be addressed to Amir Seyedkhoei; amir.khoei@gmail.com

Received 20 May 2018; Revised 22 August 2018; Accepted 29 August 2018; Published 5 March 2019

Academic Editor: Yuri S. Karinski

Progressive collapse is a persistent spread and enlargement of initial local failure of structures characterized by inconsistency between the initial failure and its resulting extensive collapse. Although, great contributions have been made towards the progressive collapse of building structures, comparably small attention has been paid to bridge structures. In this study, the procedure of progressive collapse of bridges with concrete prestressed voided slab under earthquakes and effects of other parameters on propagation of collapse of regular, semiregular, and irregular bridges are investigated. At first, a bridge specimen, which its shake table test results were provided by previous researchers, was modeled and verified using the applied element method. Then, the progressive collapse of the box girder bridge was investigated. In the next step, progressive collapse process of the same bridge with posttensioned voided slab under earthquakes was studied using nonlinear time history analysis. Irregularities of the piers were analyzed parametrically. The results show that domino-type progressive collapse happens in bridges with voided slab after the initial failure of the deck at the seating of bridge abutment. Also, it is concluded that, type of the deck, height of the piers, and ground slope have a great effect on the progressive collapse procedure of both regular and irregular bridges with voided slab deck.

1. Introduction

Since the World Trade Center towers attack (Incident New York, 2001), progressive collapse has been considered by many researchers [1]. As defined by ASCE 7-05, "Progressive collapse is the spread of an initial local failure from element to element resulting eventually, in the collapse of an entire structure or a disproportionate large part of it" [2]. Research studies conducted on progressive collapse of structures have usually focused on buildings under blast or abnormal loads, and only few studies have been conducted to investigate the vulnerability of bridges to progressive collapse induced by earthquakes, while bridge collapse usually results in huge casualties and financial losses [3].

On the other hand, due to the strategic role of bridges during the occurrence of natural disasters and their impact on relief operations, studying bridges during an earthquake is obviously important [4]. Studies conducted on the collapse of USA bridges during 1989 and 2000 (503 bridges in total) and the causes have shown that during these years, 17 bridges collapsed due to earthquakes [5]. Moreover, research on damaged bridges in China showed that the main causes of bridge collapse were poor construction, materials malfunction, earthquake-induced damage, or other dynamic excitations, weakness in maintenance, overloading of trucks, collision of ships, and bed sewage [6].

Many bridge progressive collapse incidents have occurred in history. For example, Tacoma Narrows Bridge collapsed in windstorm in 1940. In this incident, the bridge hangers were destroyed, and the failure of longitudinal beam reinforcement sheets, which obstructed the wind flow, was known to be the cause of the failure [7]. The Silver Bridge (an eyebar-chain suspension bridge over Ohio River, USA) collapsed without any alarm after 40 years of service in

December 1967 due to the failure of defective straps at node 13 on the northern side of the bridge [7]. The Viadotto Cannavino Bridge (a four-span continuous girder bridge in Italy) collapsed progressively during the construction phase in 1972, due to the collapse of the deck framework in some regions [8]. The Haeng-ju Grand Bridge (a continuous prestressed girder bridge in Seoul, Korea) collapsed progressively in 1992 during the construction. The deck cables played a major role in the bridge progressive collapse, leading to the formation of high stresses and force redistribution [8]. The I-35 W Mississippi River Bridge (a trussed bridge with a steel deck in Minneapolis, USA) collapsed progressively in 2007 as a result of the failure of the L11 and U10 connection plate in diagonal members [9].

During the dynamic destruction operation of Hongqi Bridge in Zhuzhou City, China, 9 spans of the bridge collapsed progressively due to an inaccuracy in destruction of span Number 109 [10].

Some research studies have been carried out on the progressive collapse modeling of bridges [3, 10–14]. However, very few of them have studied this kind of collapse under earthquake. Seible et al. noted that during major earthquake, continuous vibration after initial failure and repeated stress reversal from cyclic inelastic actions can lead to significant deterioration in stiffness, strength, and ductility of the structural system. These effects can lead to failure and collapse propagation [15]. In 1997, an experimental test was conducted to investigate the seismic behavior of concrete bridges. In this study, four-span bridges with different characteristics of piers reinforcement and pier height with a scale of 1 : 2.5 were fabricated in the laboratory [16]. Chiara and Rui [17] and Lau and Wibowo [3] modeled the mentioned bridge using the finite element method (FEM) and applied element method (AEM), respectively. They were able to verify the response of the bridge with experimental results. In the FEM model, the deck was modeled linearly, and its behavior was simulated using equivalent Timoshenko's beam. Lau and Wibowo utilized AEM to model and analyze the bridge at the same scale by considering linear and nonlinear deck behaviors. Finally, it was observed that in a high-level earthquake (HLE), at first, the side seating of the box girder deck failed at the abutment, then after the redistribution of force and moment, the deck failed due to punch shear at the pier supports and bridge collapse progressively. In this study, the above bridge is modeled and verified using applied element method. The purpose is to investigate the progressive collapse procedure of regular, semiregular, and irregular bridges with concrete posttensioned voided slab deck under earthquakes. Due to this, the box girder slab is replaced with the posttension voided slab. Also, different bridge samples' irregularity configuration is modeled and analyzed.

2. Applied Element Method

The applied element method (AEM) has been proved that it is a method that can simulate structure collapse behavior during all stages of load application, including the elastic stage, the beginning of cracking and its propagation in elements, the yield of steel reinforcements, the separation of components, and collision or contact of segregated elements with each other, structure, or ground [18, 19].

The structure in the AEM is modeled as an assembly of elements connected together through their surfaces with a set of normal and shear springs which represent the state of stresses, strains, and connectivity between elements.

Each 3D element has six degrees of freedoms (DOFs), three translations, and three rotations, and the deformations are also related to those six DOFs as shown in Figure 1. They can represent both concrete and steel reinforcing bars [14]. They would rupture under the following conditions:

(1) The rebar stresses reach the failure criterion, when the normal stress is equal or greater than the ultimate stress. The rebar rupture only applies to bars in tension. No cut is permitted for bars in compression.

(2) The matrix springs reach the separation strain limit. In this case, both matrix and reinforcement springs, either in compression or tension, are removed. [3].

When an element divides from the structure, it acts as a rigid body that can fall down or contact with other parts of the structure.

2.1. Material Modeling in AEM and Solving Method. The compressive concrete was modeled by the Maekawa compression model (Figure 2(a)). The modeling of concrete under tension was conducted so that the stiffness of the springs is constant and equal to the initial stiffness, until it reaches the cracking point. After cracking, the stiffness of the tension springs was considered to be zero. Moreover, for concrete springs, the relationship between shear stress and shear strain was assumed to be linear before the cracking of concrete. After the cracking, the shear stresses decreased as shown in Figure 2(b) [20].

The longitudinal and transverse reinforcements are also defined as a spring between the elements, which are modeled using the behavior provided by Ristic et al. (Figure 2(c)). Tangential stiffness of the reinforcements was calculated based on the strain of their equivalent springs, loading condition (loading or unloading), and previous situation of the steel spring that controls Bauschinger effect. The advantage of this method is that the effects of partial unloading and Bauschinger effect can be considered without any extra complexity in the analysis [21].

The method of solving dynamic equations is usually based on step by step Newmark-β method. Equations of equilibrium are in fact linear equations for each step. Equilibrium equations in AEM are usually solved by using a direct solver (upper-lower Cholesky decomposition) or an iterative solver.

2.2. Comparison of AEM and FEM. Modeling the process of progressive collapse such as the failure of elements, separation, collision of elements with each other, and elements falling on the ground is very difficult and nonfunctional in the finite element method. However, analyzing this process is very simple and operational considering the solution

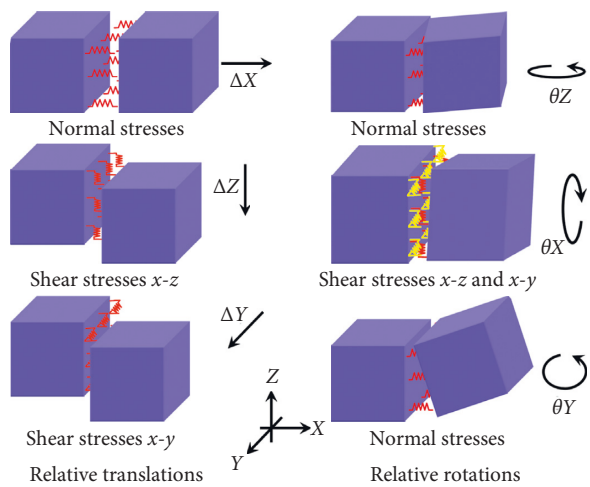

Figure 1: Translational and rotational springs in structure simulation using AEM [14].

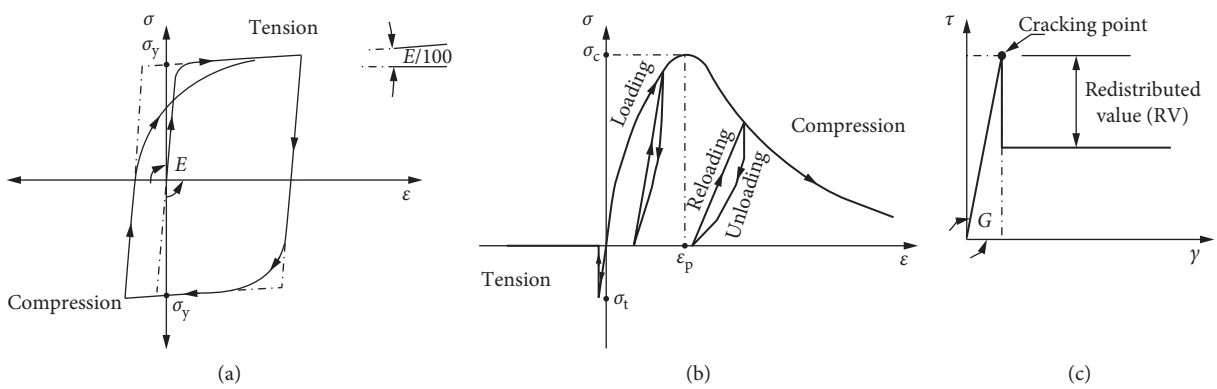

Figure 2: Constitutional curves used in AEM for concrete and reinforcements. (a) Concrete under axial stresses, (b) concrete under shear stresses, and (c) reinforcement under axial stresses [18].

method and the advantages of the applied element method. The domain and scope of AEM analysis in comparison with FEM are shown in Figure 3.

3. Simulation of the Bridge

The selected bridge (which is labeled b213) for carrying out analysis, with the scale of (1 : 2.5), has 4 span box girders of 20 m length and 5.6 m width (the full scale length and width of the deck were 50 and 14 meters, respectively). The substructure consists of three constant rectangular hollow-core reinforced concrete piers with the height of 5.6, 2.8, and 8.4 m as medium, short, and tall piers, respectively. The piers are fixed at bases, and the abutment supports are hinged (Figure 4). The piers are linked to the deck only in the horizontal transfer direction of the bridge. The reinforcement details of the bridge piers, based on their section types (Figure 5) and the material properties of concrete and steel (Table 1) were defined according to previous research. The section of first and last piers (medium and tall) is type 4 and for short pier it is type 1 [17].

In the AEM model, the bridge super structure (box girder) is modeled with both linear and nonlinear material properties in order to compare with previous analysis and pseudodynamic experimental test results. The mesh size and reinforcement details of the bridge model are selected from previous study [3] and shown in Figure 6.

The input ground acceleration of analysis is an artificial ground acceleration which had been used in pseudo-dynamic test of the sample bridge (b213) in experimental study[16]. As shown in Figure 7, the record has two peak accelerations of $0.35\,g \times 2.5 = 0.875\,g$ and $1.2 \times 0.35\,g \times 2.5 = 1.05\,g$ (g is ground acceleration), and the duration of each ground motion is $10\,s/2.5 = 4\,s$. The value, 2.5, is the scale factor of the bridge in the laboratory model, and there is 10 s gap between the two motions. This artificial record is applied in the transversal direction of the bridge [3].

3.1. Verification. After modeling the entire bridge with given details and materials, the results of nonlinear dynamic analysis by applied element method, were compared with previous research studies under first part of the record of an artificial ground motion (Figure 7) where the PGA is equal to 0.875 g and the duration is equal to 4 s. To validate the bridge model, at first, the top pier displacement was compared by considering

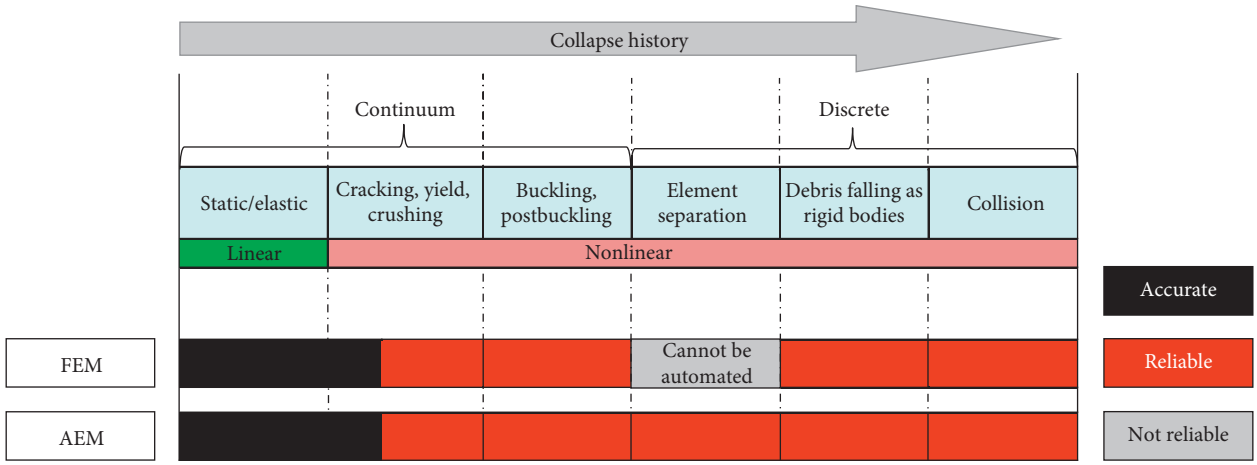

Figure 3: Comparison of analysis range between FEM and AEM.

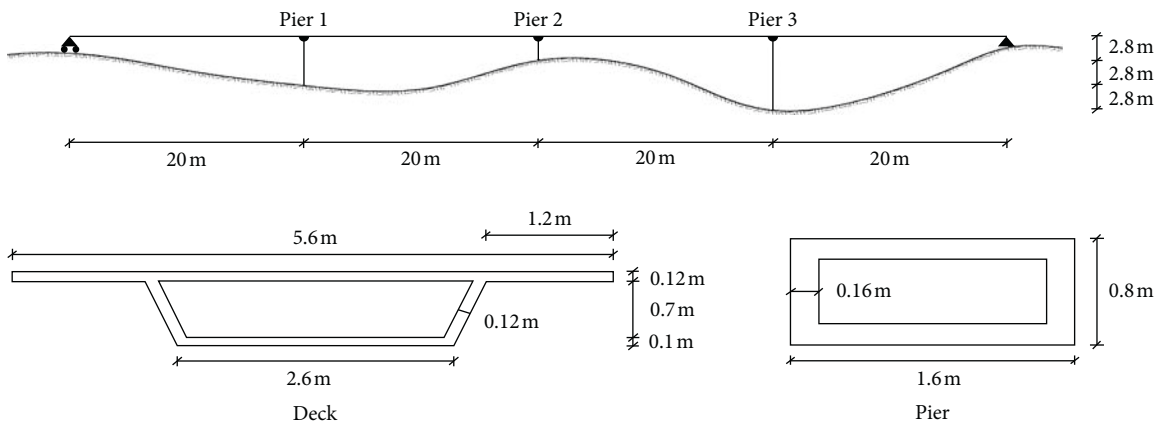

Figure 4: Longitudinal view and cross sections of b213 bridge dimensions [16], numbers 1, 2, and 3, respectively, represent short (2.8 m), medium (5.6 m), and tall (8.4 m) piers.

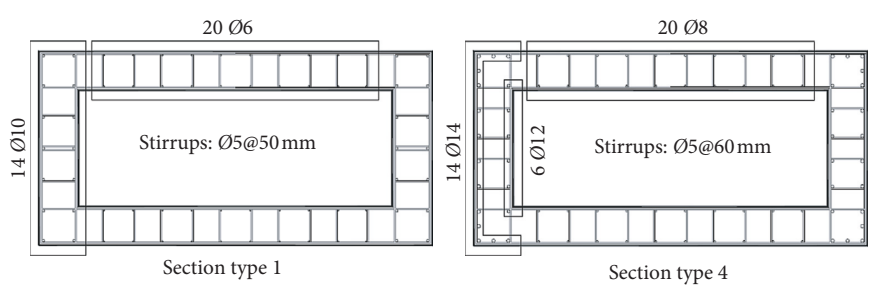

Figure 5: The reinforcement of piers section types of b213 bridge [16].

linear materials for bridge deck. After that, the bridge response was studied by assigning nonlinear behavior of the materials and reinforcement details to the box girder deck. The results for each case are explained in detail in the following sections.

3.1.1. Verification in the Case of Linear Deck. As shown in Figure 6 (diagrams a, b, and c), the top pier displacement (for short, medium, and tall piers) obtained by experimental results [17] and numerical analysis [3] in applied element method was compared with the result of the current research in AEM. As shown in the diagrams, the studied model can predict the response of bridge with a high accuracy for each pier. Moreover, the maximum piers displacements occurred at the time period of 3 to 3.5 s (the PGA of an artificial acceleration).

3.1.2. Verification in the Case of Nonlinear Deck. In this part of the research, the bridge deck was modeled nonlinearly. Also, the results of collapse procedure and the top pier displacements were compared with the results obtained by previous research [3] ((Figures 8 and 9).

Table 1: Material properties of bridge piers [17].

Parameter	Concrete			Steel
	Pier 1	Pier 2	Pier 3	
Type	4	1	4	
Compressive strength	3.212×10^6 kg/m^2	3.569×10^6 kg/m^2	4.375×10^6 kg/m^2	3.6×10^7 kg/m^2
Tensile strength	3.212×10^5 kg/m^2	3.569×10^5 kg/m^2	4.375×10^5 kg/m^2	3.6×10^7 kg/m^2
Strain at unconfined peak stress	0.002 m/m	0.002 m/m	0.002 m/m	—
Constant confinement factor	1.2	1.2	1.2	—
Young's modulus	2.549×10^9 kg/m^2	2.549×10^9 kg/m^2	2.549×10^9 kg/m^2	2.039×10^{10} kg/m^2
Shear modulus	1.062×10^9 kg/m^2	1.062×10^9 kg/m^2	1.062×10^9 kg/m^2	8.155×10^9 kg/m^2
Specific weight	2549.29 kg/m^3	2549.29 kg/m^3	2549.29 kg/m^3	7840 kg/m^3
Separation strain	0.1	0.1	0.1	0.2
Friction coefficient	0.8	0.8	0.8	0.8
Postyield stiffness ratio	—	—	—	0.01

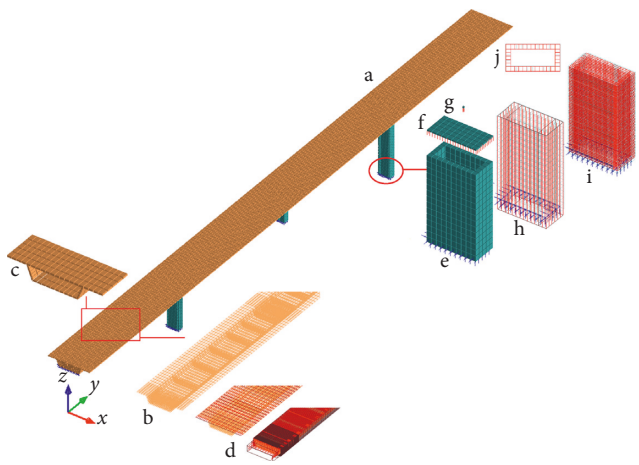

Figure 6: Bridge model in AEM: (a) hole model of bridge, (b) deck meshing overview, (c) deck section, (d) deck reinforcing, (e) pier section and its meshing details, (f) elastic plate to better load distribution on pier, (g) pin element, (h) longitudinal reinforcement, (i) transverse reinforcement, and (j) stirrups details.

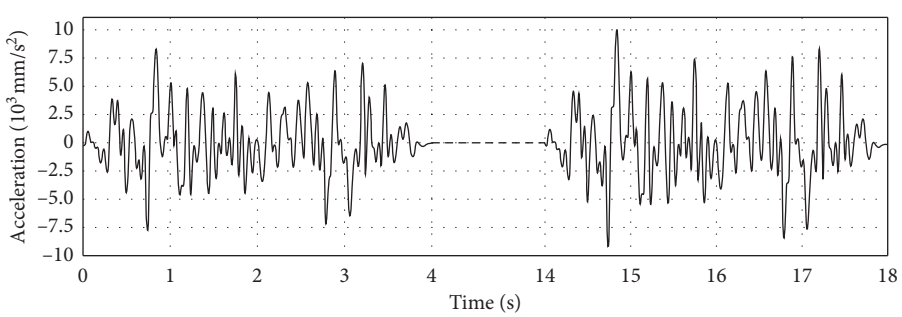

Figure 7: An artificial ground motion [16].

Collapse procedure of b213 bridge in the case of nonlinear deck in AEM according to the current study is similar to that of the research conducted by Lau and Wibowo [3] using the same method of analysis. In this case, at first, the box girder fails from abutment, and then the gravity forces redistribute to the pier bearings. After that, box girder experiences shear failure due to punching on pier bearings and by this way, the entire bridge collapses progressively. With these results, it can be concluded that the bridge nonlinear model, including piers details, deck dimensions, reinforcement details and also materials, is done correctly.

Based on the obtained results, the bridge responses in AEM under the artificial ground motion, matched accurately with the shake table test results of the bridge with linear deck properties. The Lau and Wibowo results were used in order to validate the boundary conditions, nonlinear behavior, meshing details, and reinforcement details of the box girder deck, in seismic response of the bridge in AEM. By using this

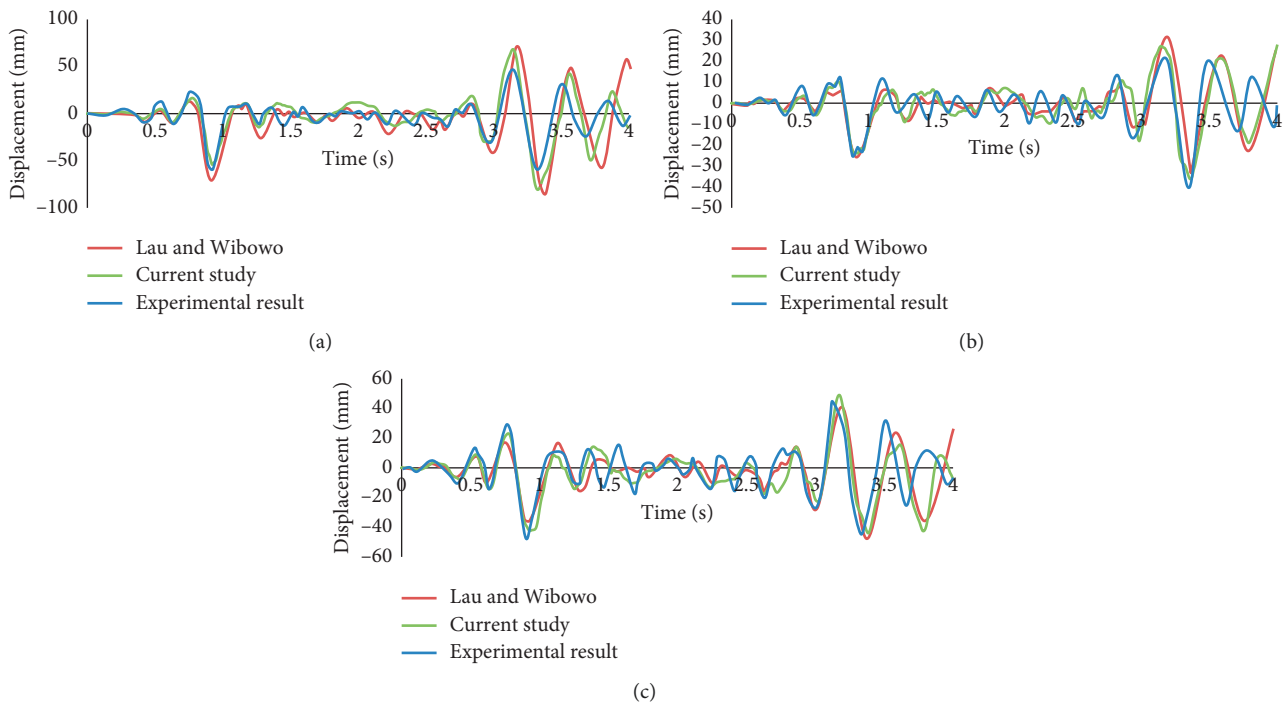

Figure 8: Comparison of the response of the bridge (b213) (linear box girder) in the current research, with the research of Lau and Wibowo [3] and experimental study [17] for (a) short, (b) medium, and (c) tall piers.

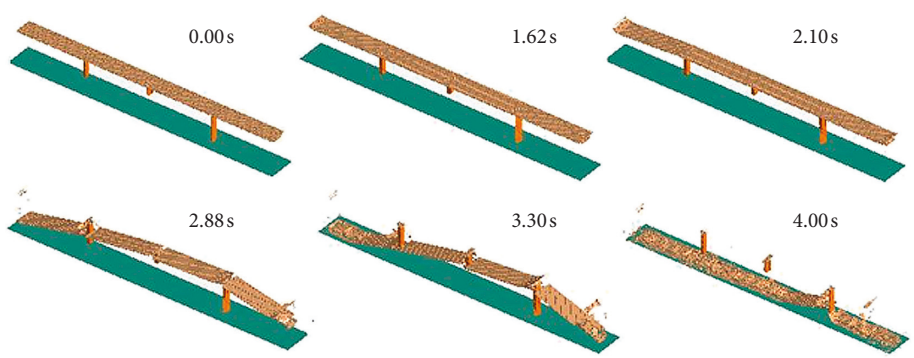

Figure 9: Collapse procedure of B213 bridge in the case of nonlinear deck in AEM, according to the current study.

validation results, the progressive collapse behavior of the sample bridge with voided slab, or with different pier placement, would be more reliable.

4. Progressive Collapse of Posttensioned Voided Slab

Previous research studies showed that concrete voided slab might be more vulnerable in domino-type progressive collapse, after the initial failure of the deck [10]. In this part of the study, by utilizing the verified bridge model in previous sections, the posttensioned voided slab was replaced with box girder and the nonlinear dynamic behavior of the progressive collapse of the new bridge model was investigated in AEM. For this purpose, the main properties of concrete voided slab such as weight, moments of inertia, etc., should accurately match with concrete box girder. Comparison of the properties of concrete voided slab with the concrete box girder deck is shown in Figure 10 and Table 2.

In order to ensure that the moments of inertia in voided slab and box girder are the same, as well as to reduce the weight of voided slab, the width of the slab was considered to be shorter than that of the box girder width as much as possible until the moment of inertia about axis 3 is equal in both types of decks. However, the cross section areas of two deck sections would still not be the same, and this discrepancy leads to a difference in their weight. Thus, in order to maintain mechanical properties of cross sections of two types of deck and the verification of the piers, the concrete density of the voided slab was reduced, and the weighs of both decks became the same. In this case, the design forces of the piers did not change, and the validated piers in the case of box girder deck were also valid in voided slab deck (Figure 11).

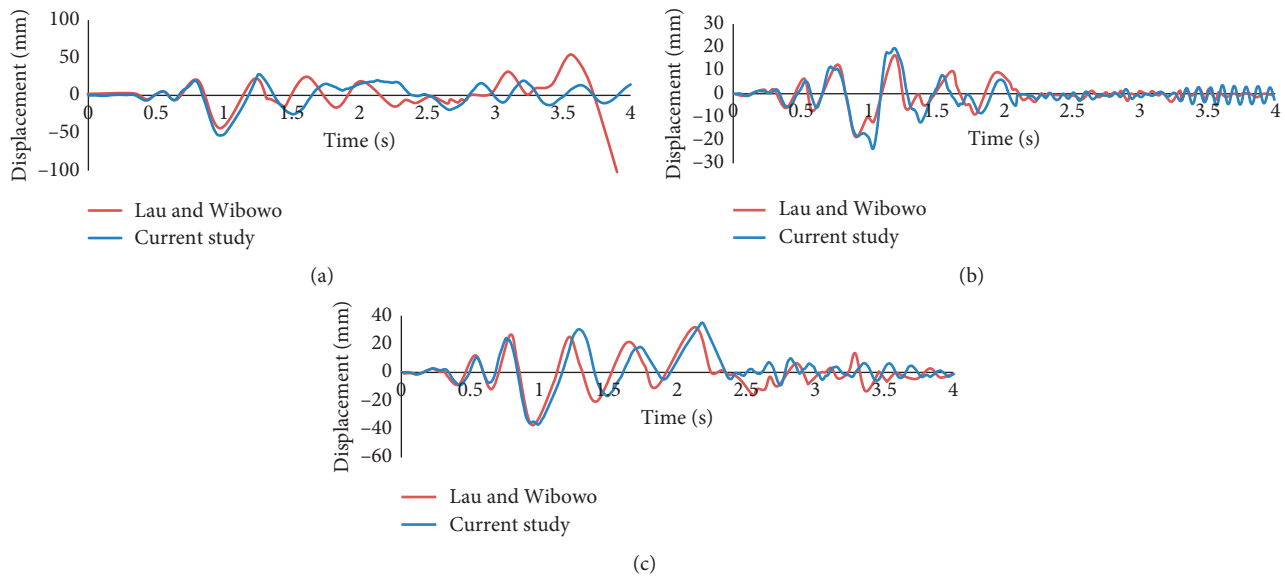

Figure 10: Comparison of the displacement response of bridge b213 piers with nonlinear deck using AEM in the current study, and Lau and Wibowo [3] research: (a) short, (b) medium, and (c) tall pier.

Table 2: Comparison between box girder and voided slab decks' cross sectional properties.

	Box girder	(Prestressed) voided slab
A (Area gross section (m^2))	1.110	1.629*
Torsion constant (m^4)	0.323	0.331
Moment of inertia about 3 axis (m^4)	0.133	0.133
Moment of inertia about 2 axis (m^4)	2.251	2.248

*Modified with reduction in concrete density.

5. Progressive Collapse of Regular and Irregular Bridges

5.1. Selection of Regular, Semiregular, and Irregular Bridges. To investigate the effect of number of spans and pier irregularity on progressive collapse procedure of posttension voided slab bridges, the regular, semiregular, and irregular bridges were selected as shown in Figure 12 based on conducted studies [22]. The regularity criterion for bridges is defined based on AASHTO (Table 4.7.4.3.1-2—Regular Bridge Requirements) [23].

5.2. Ground Motions of Regular and Irregular Bridges. Four ground accelerations are used in this part of study to investigate the regularity effect of bridge piers. The first one is an artificial ground motion which has 18 seconds duration and selected from the shake table test on the sample bridge [16] to verify the b213 bridge response. All the bridges in Figure 12 are analyzed under the artificial ground motion. Also to evaluate the seismic manner of different types of bridges under real earthquakes, the other three ground motions are obtained from the Pacific Earthquake Engineering Research (PEER) Strong Motion Database. These records are selected because some bridge collapses have been reported during them. In order to reduce the calculation's volume, the b2222222, b123, and b2331312 bridges are analyzed as regular, semiregular, and irregular bridges, respectively, under Kobe 1995, Chi-Chi 1999, and Northridge 1994 ground motions, and their details can be seen in Table 3. All the real records are scaled to scale factor of bridge models (scale factor = 2.5).

5.3. Mechanism of Collapse. According to the selected bridges (regular, semiregular, and irregular), to assess the collapse process and also due to the variability in piers height, a factor named R, which is pier height to span length ratio, was used. The reason for using such factor is classification of collapse type for each pier.

$$R = \frac{H}{L}, \tag{1}$$

where H is height of pier which has three values (2.8, 5.6, and 8.4 m) and L is the length of span for all bridges in all spans which is constant and equal to 20 m. Thus, the bridge piers can be divided into three groups based on the ratio of R as shown in Table 4. The collapse propagation method in the current study can be classified by the R ratio of bridge piers into three mechanisms.

First type mechanism occurred in the bridges and their piers are considered in group 1 ($R > 0.4$). In this case, after the

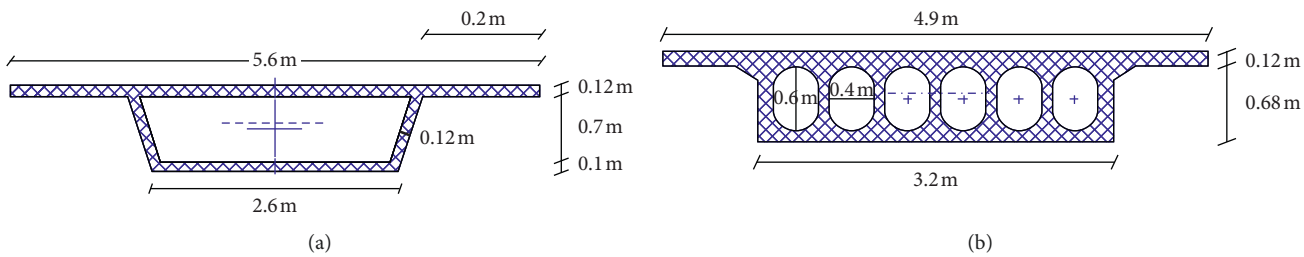

Figure 11: Cross section: (a) box girder; (b) posttensioned voided slab.

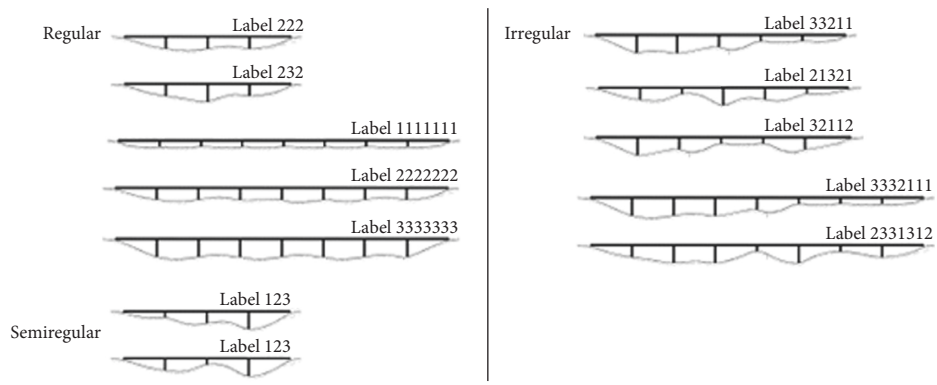

Figure 12: Bridge configurations [22]. Numbers 1, 2, and 3 in the name of bridges (for example b213), respectively, represent short (2.8 m), medium (5.6 m), and tall (8.4 m) piers. The length of span in all bridges is 20 m.

Table 3: Summary of earthquake ground motions.

Earthquakes	Station	Magnitude	Pick ground acceleration (g)	Pick ground velocity (cm/s)	Pick ground displacement (cm)
1994 northridge	Newhall fire station	6.7	0.63	101	36
Kobe 1995	Kobe (JMA)	6.9	0.85	105	26
Chi-Chi 1999	TCU076	7.6	0.41	88	129

failure of the deck support in abutment, it fell down and collided with the ground, the other side of the deck fracture at about 0.1 length of the deck, and separated deck was imposed with the adjacent pier which resulted in shear load several times more than shear capacity of the pier and hence, the pier collapse. This procedure continued progressively until the complete collapse of the bridge occurred. According to progressive collapse typology, this kind of collapse propagation is considered as the domino-type progressive collapse [24]. For example, b3333333 bridge progressive collapse is considered as the first type of progressive collapse and its details and procedure are shown in Figure 13(a). This procedure in comparison with a real incident is shown in Figure 13(b). In this mechanism of collapse, due to the collision of deck with pier, the high amount of shear force in a short period of time is applied to the pier (Figure 14).

Second type mechanism occurred in the bridges and their piers are considered as group 2 ($R < 0.2$, short piers). In this type of progressive collapse, after the failure of the deck at the connection of deck and abutment, it falls down and collides with the ground. Due to the large rotation of the deck, it fractures at the distance of 0–0.1 L (L = length of the span) in adjacent span, and because of that, there is no impact in this form of collapse. The collapsed deck remains stable on pier support diagonally, and this procedure continues progressively until the entire bridge collapses. For example, progressive collapse of b2222222 bridge is similar to second type mechanism of collapse. Steps and details of this procedure are shown in Figures 14 and 15.

Table 4: Different groups of piers based on pier height to span length ratio.

Group number	$R > 0.4$ 1	$R < 0.2$ 2	$0.2 < R < 0.4$ 3

Third type mechanism occurred in the bridges and their piers are considered as group 3 ($0.2 < R < 0.4$). It can be also called combined mechanism. In this case, the collapse propagates with both mechanisms of first and second types. Steps and details of this procedure are shown in Figure 16.

By considering these concepts and categories, the progressive collapse procedure of the bridges presented in Table 4, is explained by their regularity. It should be considered that in all the bridges, the fracture is initiated from the

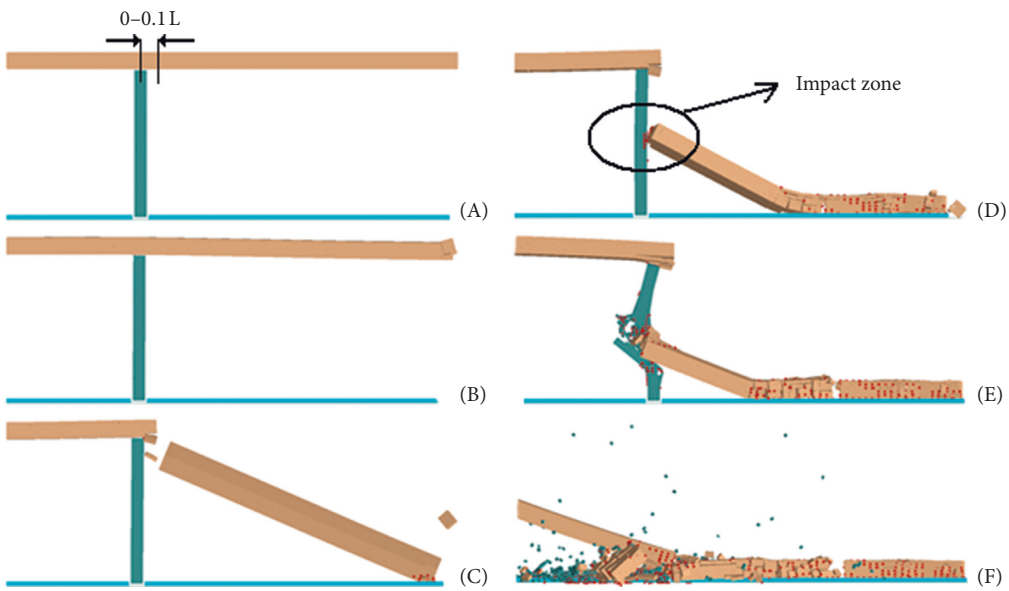

(a)

(b)

Figure 13: First types of progressive collapse of bridges (domino-type progressive collapse) (a) in analysis: (A) stable condition, (B) initial crack in abutment support, (C) falling down of the first span deck on the ground, (D) collision of the other side of the deck with pier, (E) shear fracture of pier and instability of second span, and (F) complete collapse of first span; (b) in practice.

abutment and moves towards the piers; however, it is not the certain rule and the initial failure that can be started from any location but in this study, and for analysis of the important factors in progressive collapse of regular and irregular bridges, the strength of the connection of the deck and the abutment was considered to be less than other part of the deck. In fact, in this study, causes of initial failures are not important, and only the collapse propagation and practical ways to prevent this phenomenon is the main purpose.

5.4. Results

5.4.1. Regular Bridges under the Artificial Earthquake. The results of the nonlinear dynamic analysis of regular bridges using AEM (Figure 16) show that, the b3333333 bridge (with tall piers) which is considered in group 1($R > 0.4$) completely collapses by first type mechanism of progressive collapse (domino-type progressive collapse). In the b1111111 bridge (with short piers), which is considered in group 2 ($R < 0.2$), collapse propagation in all spans occurs with second mechanism of progressive collapse. And finally, in bridges with medium piers (b222, b2222, b222222, and b2222222) considered in group 3 ($0.2 < R < 0.4$), collapse occurs with

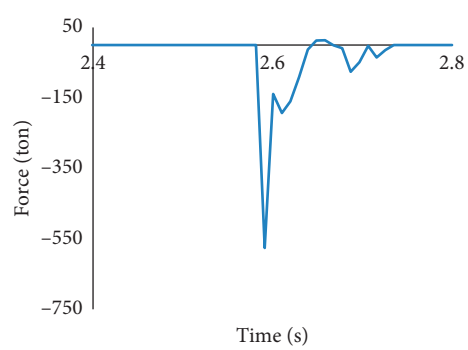

Figure 14: Impact force due to collision of deck with pier.

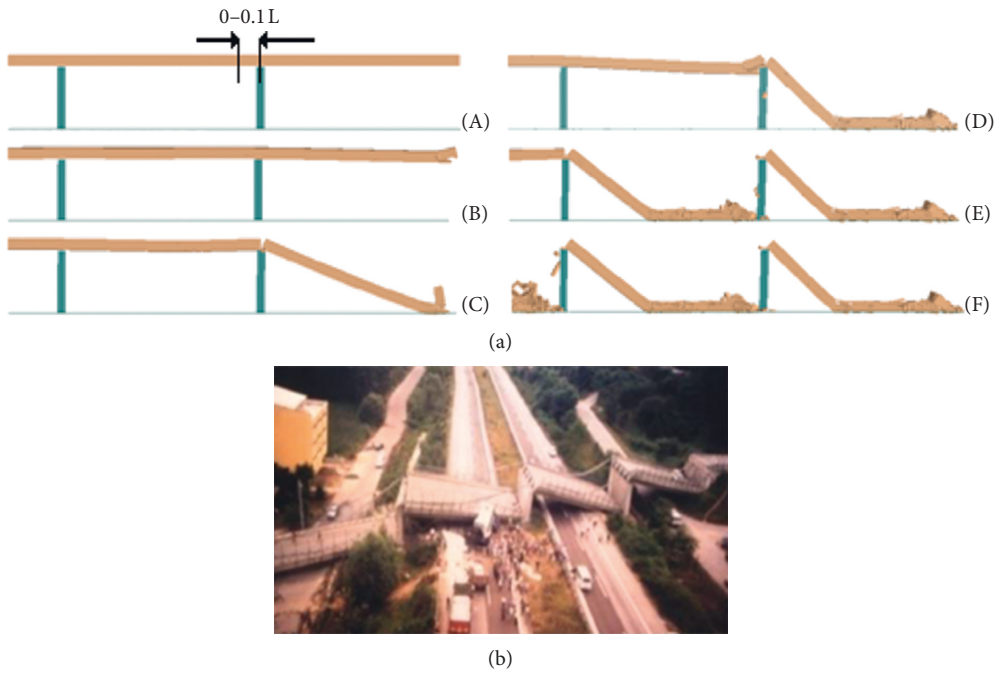

Figure 15: Second type of progressive collapse of bridges (a) in analysis: (A) stable condition, (B) initial crack at the connection of deck and abutment, (C) falling down of the first span deck on the ground and large rotation of deck at pier bearing, (D) fracture of adjacent span at distance of 0–0.1 L (E) the same mechanism occurring for adjacent span, and (F) propagation of collapse in the bridge; (b) in practice.

second mechanism in most spans. But totally, this group is considered as group 3 in which both mechanisms of collapse are likely to occur (like b222's first span, which collapses with first mechanism (Figure 16).

5.4.2. Semiregular and Irregular Bridges under the Artificial Earthquake. In this section, progressive collapse in semiregular and irregular bridges (b213, b123, b33211, b21321, b32112, b2331312, and b3332111) under an artificial ground motion was examined using nonlinear dynamic analysis in AEM. On these bridges, the process of progressive collapse is presented in Figure 17. It is shown that in semiregular and irregular bridges, the height of the piers varies. Totally, the bridge with different pier height is placed in group 3 ($0.2 \leq R \leq 0.4$); both mechanisms of progressive collapse are probable for them.

5.4.3. Regular, Semiregular, and Irregular Bridges under the Real Earthquakes. In this part of study, b2222222, b213, and b2331312 are selected as regular, semiregular, and irregular bridges respectively. The domino progressive collapse probability of the bridges was investigated under the real earthquakes of Northridge (1994), Kobe (1995), and Chi-Chi (1999) based on Table 3. The results are shown in Figure 18.

For b2222222 bridge, under Kobe earthquake, the damage started from abutment and the fallen span impact with the pier and collapse propagated with this domino-type mechanism until the bridge collapsed completely. The collapse process of this bridge under Northridge and Chi-Chi earthquakes started like Kobe earthquake, but in the middle of the analysis, the remaining parts of the bridge became unstable, and 3 to 4 spans collapsed suddenly. For b213 bridge, due to pier variation, the bridge spans collapsed with both mechanism under different earthquakes. For b2331312 bridge, like b213 bridge, the collapse propagated with both mechanism. In this bridge under Chi-Chi earthquake, the progressive collapse has been stopped at fourth span which seems that due to the ground slope the deck did not impact with pier.

The results of these parts show that the regular, semiregular, and irregular bridges with concrete posttensioned voided slab, under real earthquakes, after the failure of any sections of the bridge, the damage might expand progressively by both mechanism of collapse.

5.4.4. Imposed Impact Force. As shown in Figure 13, after the collision of the deck with pier, the shear failure occurred in pier due to high amount of impact force and low shear capacity of pier.

The shear strength of the reinforced concrete (RC) pier can be calculated by V_n. Different design codes such as the ACI Building Code [25] and AASHTO specifications [23] offer shear strength of (RC) piers consisting of concrete contribution (V_c) and steel contribution (V_s), and finally V_n is given as follows:

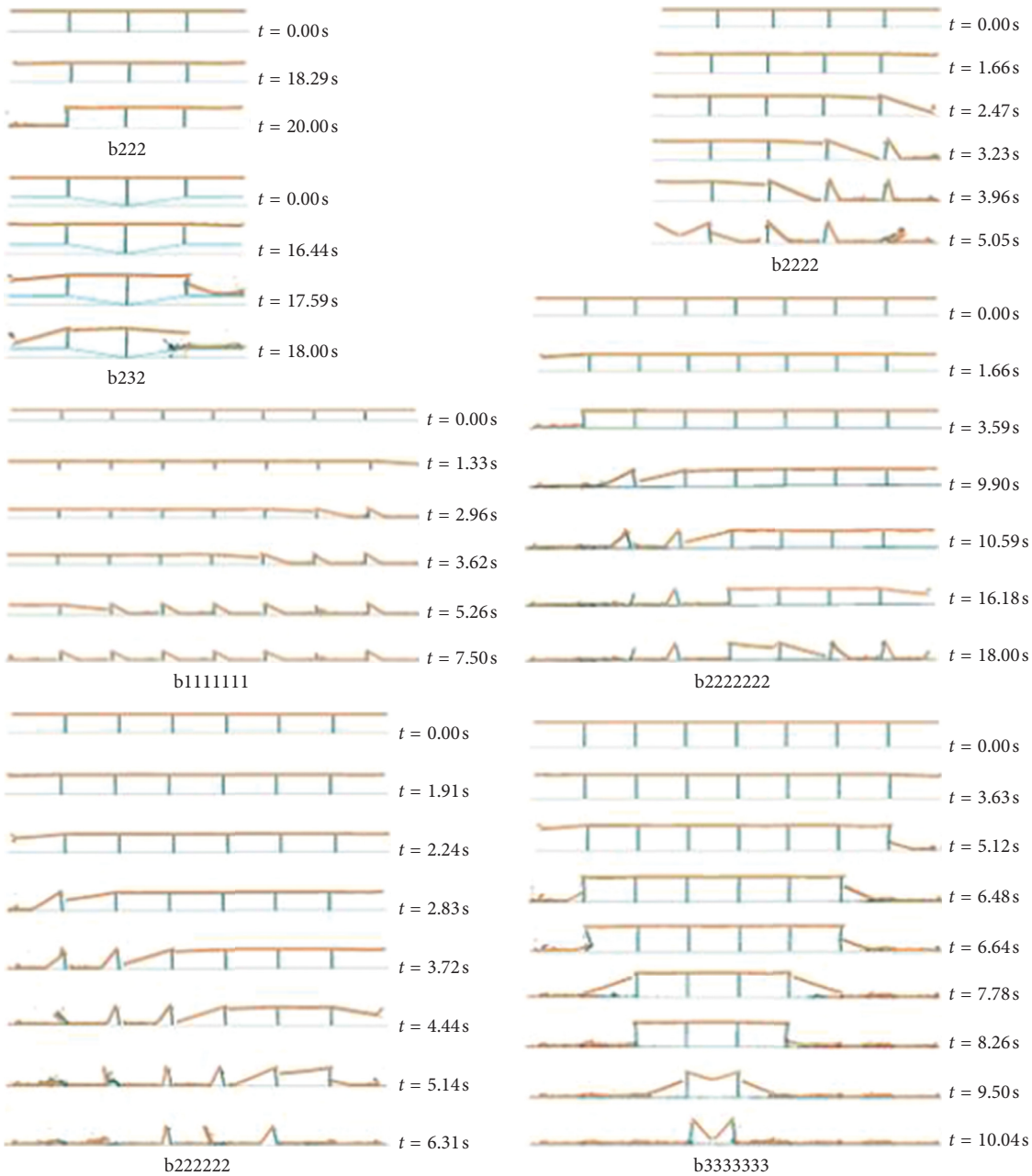

Figure 16: Collapse process of regular bridges under the artificial earthquake.

$$V_n = V_c + V_s, \tag{2}$$

where

$$V_c = 2\left(1 + \frac{P}{2000A_g}\right)\sqrt{f_c}b_w d\,(\text{lbs}), \tag{3}$$

$$V_s = \frac{A_v f_{yh} d}{s} \tag{4}$$

where in Equation (3), P is the axial load (in lbs), A_g is the gross cross-sectional area (in in^2.), f_c is the compressive strength of concrete (in psi), b_w is the width of the section (in inches), d is the distance from the extreme compression fiber to centre of the tension reinforcement area (in inches), and in total, $b_w d$ can be taken as $0.8A_g$. In Equation (4), A_v is the transverse steel area, f_{yh} is the yielding strength of the transverse steel, d is the distance from the extreme compression fiber to centre of the tension reinforcement area (in inches), and s is the vertical distance between hoops.

With regards to Equations (2)–(4), for two types of cross sections of piers (Figure 5), the V_c, V_s and the nominal shear strength (V_n) are given in Table 5.

It should be noted that the shear capacity of the piers at the moment of impact is obtained by considering half weight

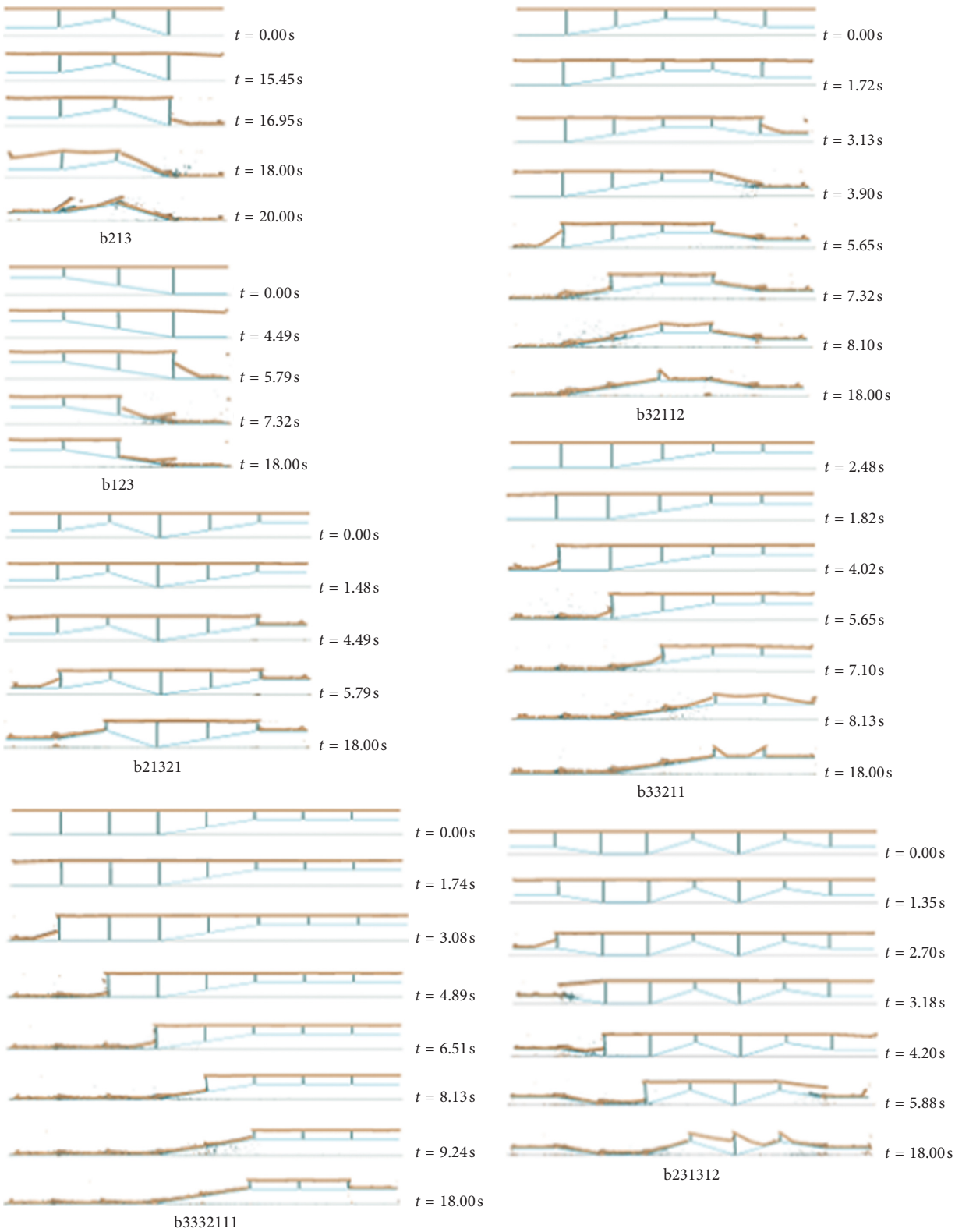

Figure 17: Collapse process of semiregular and irregular bridges under the artificial earthquake.

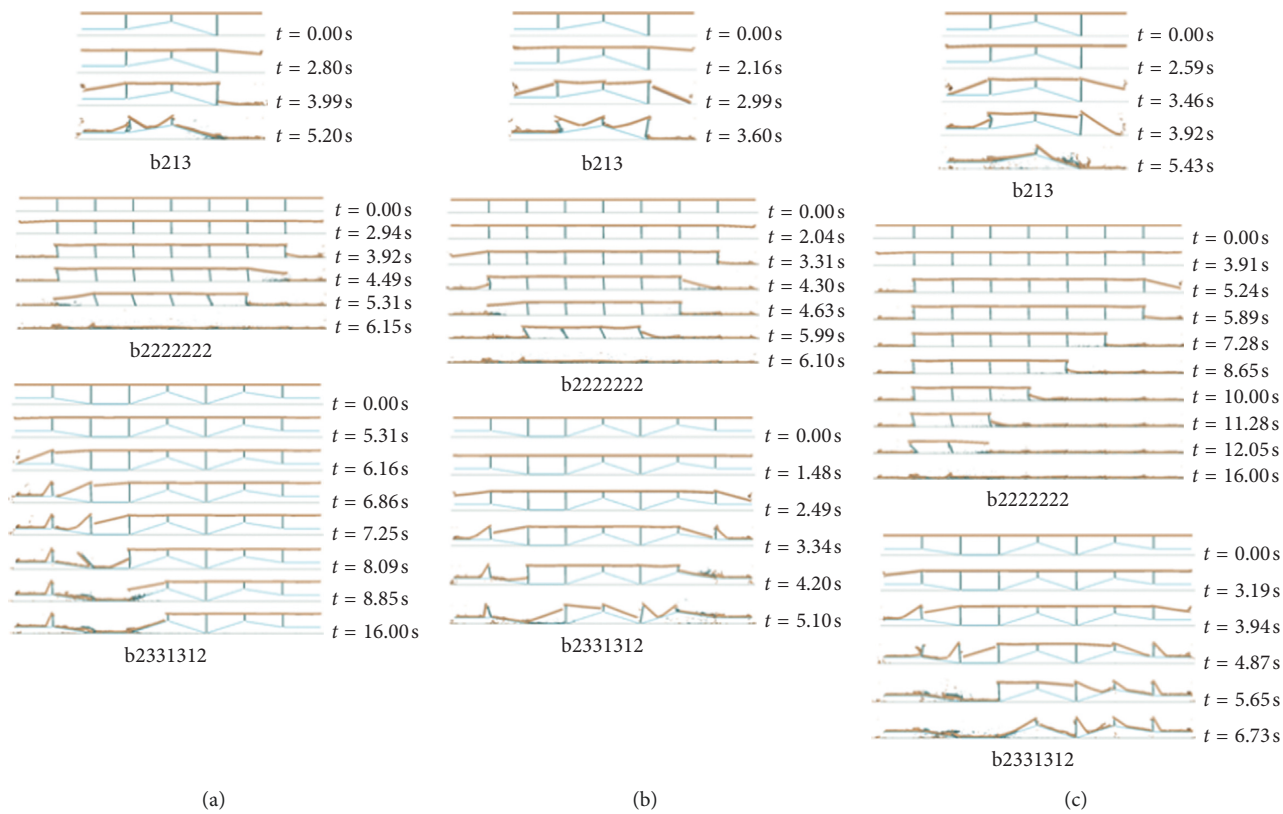

Figure 18: Collapse process of regular, semiregular, and irregular bridges (b2222222, b213, and b2331312, respectively) under (a) Chi-Chi earthquake, (b) Northridge earthquake, and (c) Kobe earthquake.

Table 5: Shear strength of the bridge section type of piers.

	V_c (ton)	V_s (ton)	V_n (ton)
Section type 1	58	47	105
Section type 4	58	37	95

of the span because in domino progressive collapse, the falling span should be neglected in calculating the axial load. In fact, it is a slight underestimation of the actual nominal shear strength of the bridge pier, because when the slab of the previous span imposed with the pier, it generates both vertical impact force through the angel of the deck and also a vertical force through friction of the falling span with the pier. However, in practice, because of the poor understanding of the dynamic variation of shear strengths in concrete and steel, it is usually better to be neglected.

As shown in Figures 19–21 which is the analysis results of bridges under the artificial and real earthquakes, by doing quantitative comprehensions between the shear capacity of the bridge piers with the base shear due to seismic loads and impact force because of deck collision, it is concluded that the seismic base shear of the pier have a direct relation with its stiffness, but the impact force is several times more than its shear capacity.

Also, it is conducted that in bridges with the same sections and length of the spans, under the same ground motion, the higher the height of the pier, the more impact force would be applied Figure 22.

Another important point is the location that the deck imposed with the pier, which in regular bridges, is located at a distance of zero to 40% of the pier height from the foundation. But in semiregular and irregular bridges, it is not easy to predict the approximate region of the deck-to-pier collision. In the case of irregular bridges, there is no specific rule to find the exact place of impact on piers due to effect of other factors like the ground slope and height of pier.

5.5. Ground Slope Effects. By investigating the sample bridges of this study, it is concluded that in the piers that ground slope makes an obtuse angle; the possibility of a deck-pier collision or a severe impact force will be reduced. In fact, in the valley bridges, where the ground topography is similar (Figure 23(a)), it can be estimated that the collapse procedure in the bridge structure will be stopped. In contrast, when the ground and pier make an acute angle (Figure 23(b)), the impact possibility increases and also, the impact force will be more severe in comparison with the normal condition of ground slope (Figure 23(c)). Therefore, in the irregular bridges, the ground slope can prevent the collapse propagation, for example, in the case of bridge B3332111, between piers 4 and 5. The ground slope, however, intensifies the impact force in some other cases like b2331312-pier2.

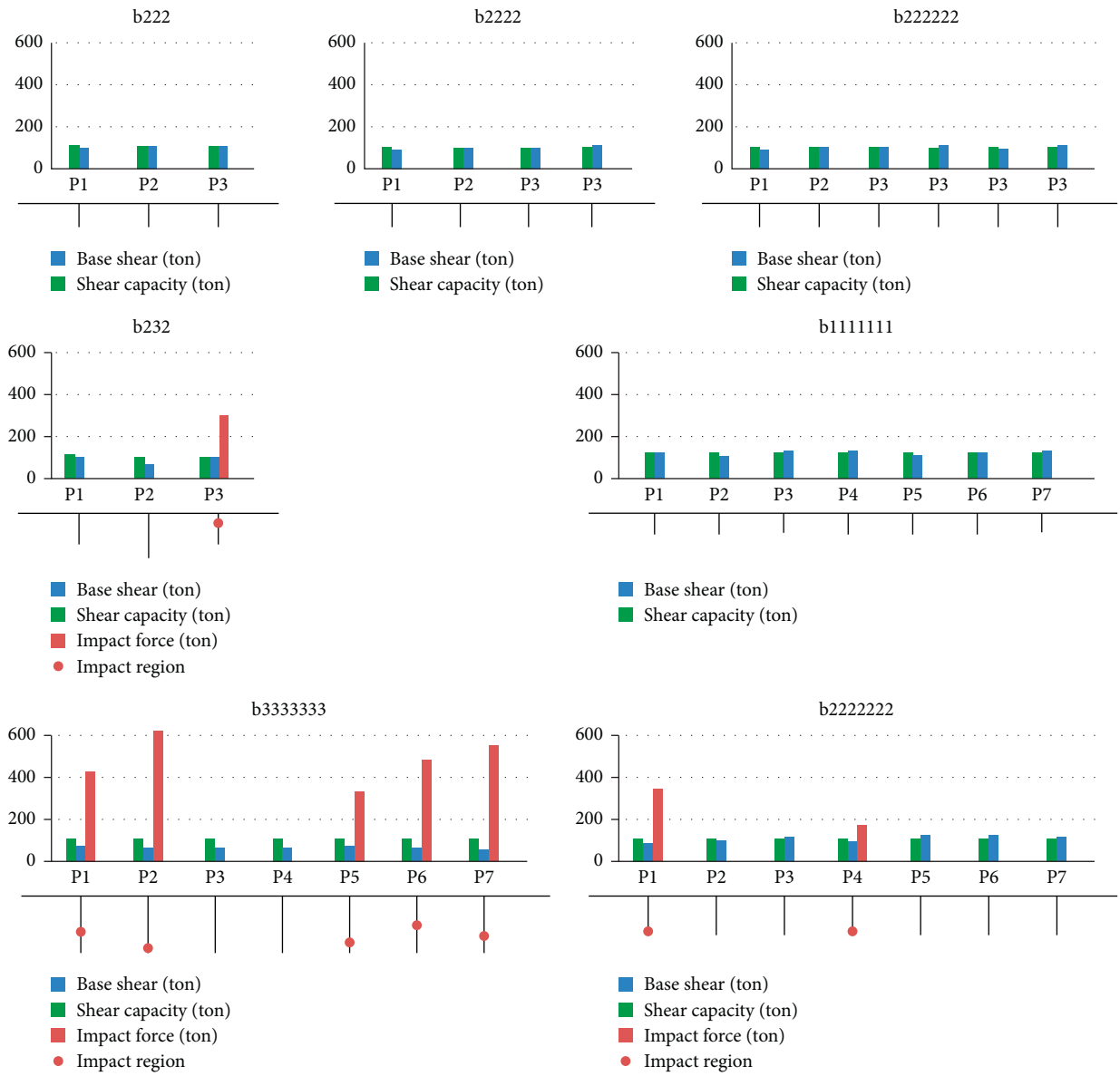

Figure 19: General information and overall view of comparing impact force with seismic base shear and the collision region in regular bridges under the artificial ground motion.

5.6. Pier Height Effects. Figure 23 presents the impact force value for short, medium, and tall piers in regular and irregular bridges, and it can be concluded that in the both types of bridges, the collision possibility and its severity will increase when the pier height increases. This can be attributed to the high potential energy of the decks at high elevations.

5.7. The Number of Spans Effect. By considering regular and irregular bridges, it can be concluded that with the increase in the number of spans, the probability of collapse initiation will increase. For example, in 4-span bridges, the deck starts to fail at second peak acceleration of the artificial earthquake record; in contrast, in more than 6-span bridges, the connection of the deck breaks down at first peak acceleration, which is 20% less than the first peak acceleration.

6. Conclusion

According to the study conducted on sample bridges, the following conclusions were drawn:

(i) The progressive collapse of bridges with concrete posttensioned voided slab deck under seismic loads mostly occurs by domino-type, while in bridges with concrete prestressed box girder slab, punching occurs on the seating regions of the box girder.

(ii) The results show that by using single pier due to its low redundancy as a substructure of bridges, the possibility of progressive collapse increases with the occurrence of an initial failure.

(iii) Progressive collapse occurs in regular, semiregular, and irregular bridges, but the prediction of the

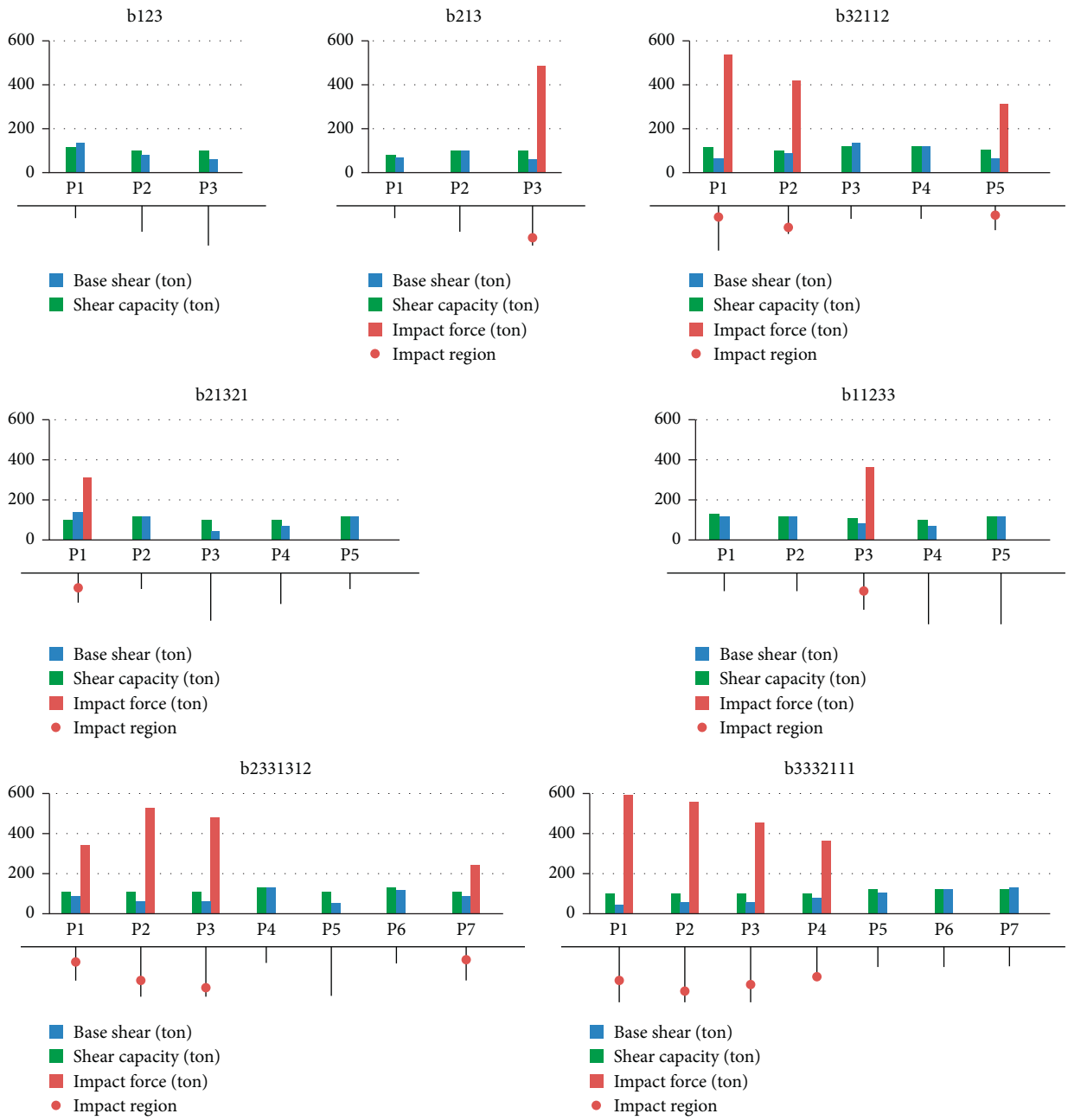

Figure 20: General information and overall view of comparing impact force with seismic base shear forces and the collision region in semiregular and irregular bridges under the artificial ground motion.

mechanism of progressive collapse in regular bridges is far easier than semiregular and irregular bridges, due to the effect of various factors such as ground slope, different piers height when compared, the exact location of initial failure, and direction of collapse propagation in semiregular and irregular bridges.

(iv) In the study on regular and irregular bridges, it was concluded that the height of the piers had a great influence on the progressive collapse mechanism, and most of the tall piers and some of the medium piers collapsed due to the deck-to-pier collision (first mechanism and domino-type progressive collapse), while the short piers as well as some medium piers collapsed due to the bending failure of the next span of the deck (second mechanism).

(v) Compression between impact force and shear capacity of the pier shows that piers can survive without severe damage in design earthquake (PGA = 0.875 g) but the impact force due to deck-to-pier collision is several times more than the shear capacity and hence, it is not reasonable to design the pier for this amount of force. It is better to prevent collapse propagation or deck-to-pier collision with other alternatives.

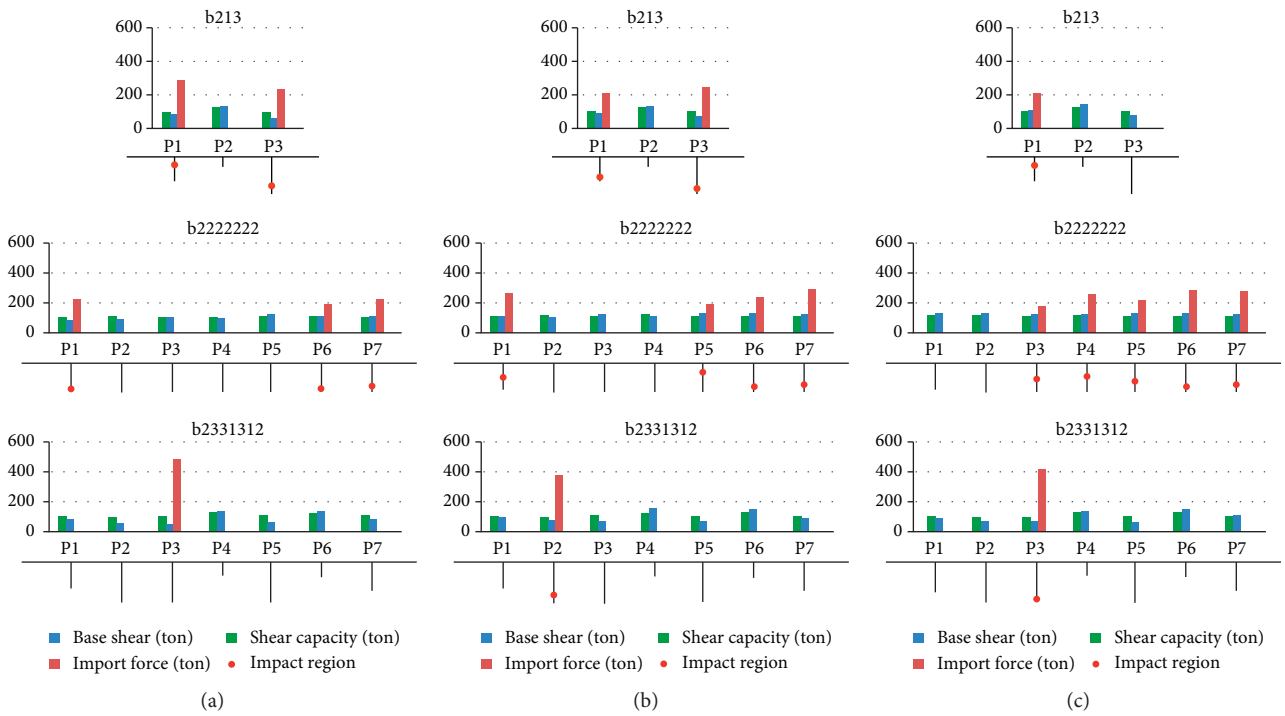

Figure 21: General information and overall view of comparing impact force with seismic base shear forces and the collision region in b213, b222222, and b2331312 bridges under (a) Chi-Chi earthquake, (b) Kobe earthquake, and (c) Northridge earthquake.

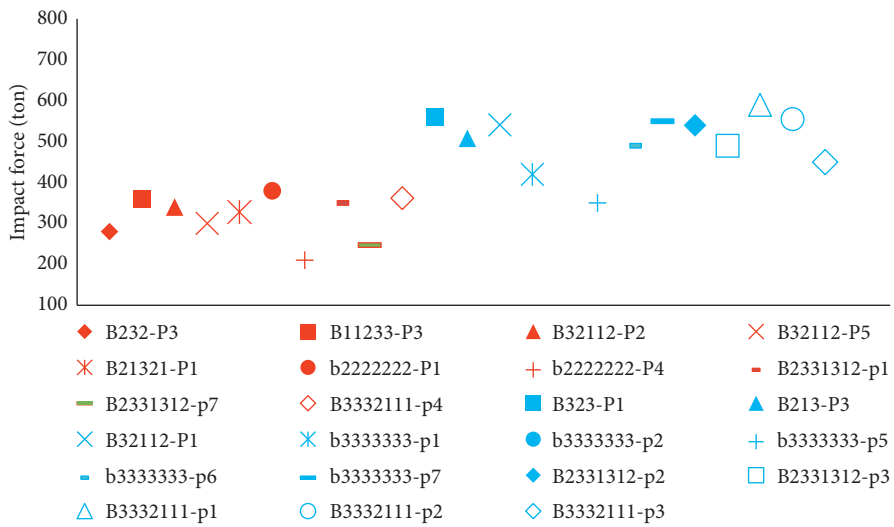

Figure 22: Impact forces for different types of piers (all red marks represent medium piers and all blue marks represent tall piers). ∗B232-p3 means pier 3 of b232 Bridge.

(vi) In the analysis of bridges with different pier elevations, it was concluded that the ground slope has a significant effect on propagation of collapse, and in fact, if the cosine of the angle between the ground slope and the pier has a positive value (an acute angle), the probability of the impact will increase as compared to the usual case (without slope). However, in the case where the cosine of the angle has a negative value (an obtuse angle), the ground slope deters progressive collapse from propagation. It should be noted that the angle of the ground and the pier should be calculated in the collapse propagation direction.

(vii) The AM (applied element method) was proven to be a very good numerical tool that can be used to analyze and investigate progressive collapse of regular, semiregular, and irregular bridges.

(viii) In all the imposed impact piers that are investigated in this study, it is observed that the

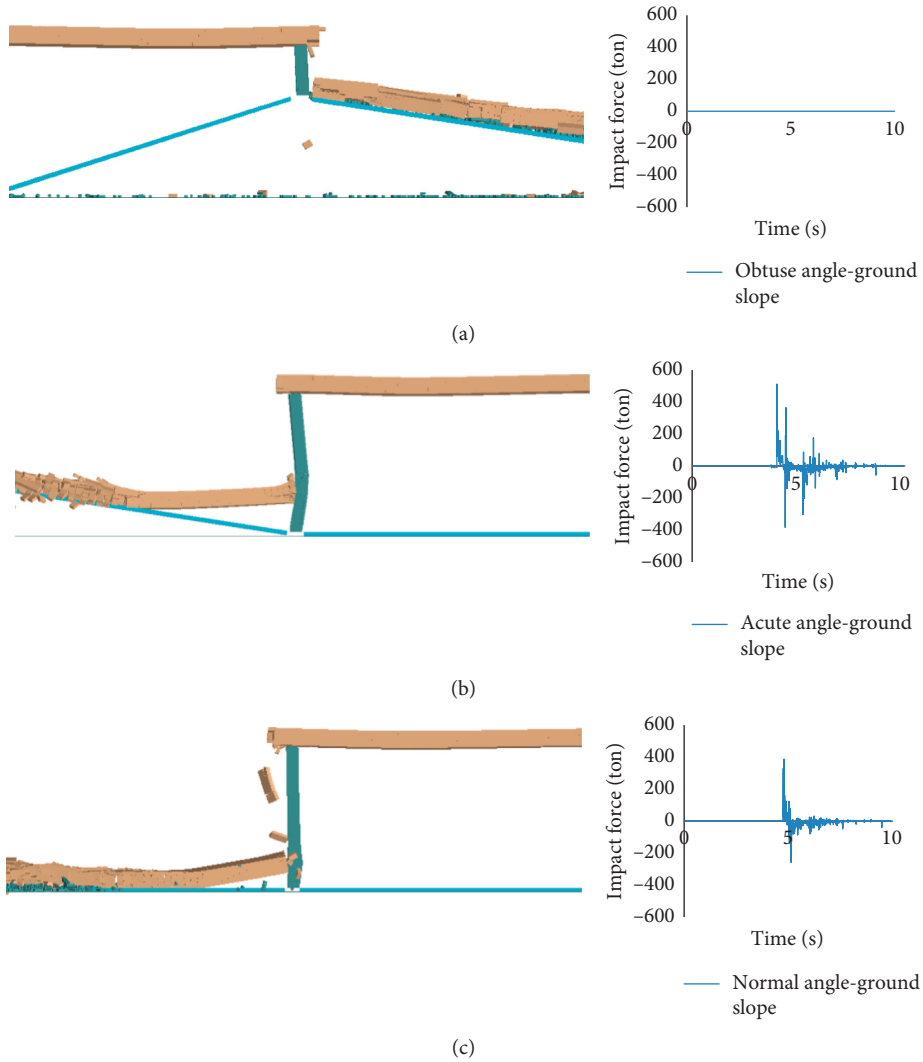

Figure 23: Effect of ground slope on impact possibility and collapse propagation: (a) obtuse angle, (b) acute angle, and (c) normal angle.

average values of impact forces in the medium piers are less than those of the tall piers. In fact, the height of the piers has a direct relation with the amount of impact force.

(ix) In regular, semiregular, and irregular bridges with concrete prestressed voided slab, under real earthquakes (Kobe, El Centro, and Northridge), with the occurrence of crack and failure in abutments, collapse is propagated in length of bridge by first (domino-type) and sometimes, second type of progressive collapse.

The researchers suggest that study on reasonable alternatives that can prevent collapse propagation in strategic bridges should be conducted in the future.

Data Availability

The data used to support the findings of this study are available from the corresponding author upon request.

Conflicts of Interest

The authors declare that they have no conflicts of interest.

Acknowledgments

The authors would like to thank Dr. A. Gharighoran for his helps and advice in editing the revised paper according to the referees' comments..

References

[1] U. Starossek, "Progressive collapse of bridges—aspects of analysis and design," in *Proceedings of International Symposium on Sea-Crossing Long-Span Bridges*, Mokpo, Korea, February 2006.

[2] ASCE: 7-05, *Minimum Design Loads for Buildings and Other Structures*, American Society of Civil Engineers (ASCE), Reston, VA, USA, 2005.

[3] D. T. Lau and H. Wibowo, "Seismic progressive collapse analysis of reinforced concrete bridges by applied element method," in *Earth and Space 2010: Engineering, Science,*

Construction, and Operations in Challenging Environments, pp. 3019–3026, American Society of Civil Engineers, Reston, VA, USA, 2010.

[4] L. Deng, W. Wang, and Y. Yu, "State-of-the-art review on the causes and mechanisms of bridge collapse,"*Journal of Performanceof Constructed Facilities*, vol. 30, no. 2, Article 04015005, 2015.

[5] K. Wardhana and F. C. Hadipriono, "Analysis of recent bridge failures in the United States," *Journal of Performance of Constructed Facilities*, vol. 17, no. 3, pp. 144–150, 2003.

[6] F. Y. Xu, M. J. Zhang, L. Wang, and J. R. Zhang, "Recent highway bridge collapses in China: review and discussion,"*Journal of Performance of Constructed Facilities*, vol. 30, no. 5, Article 04016030, 2016.

[7] A. G. Lichtenstein, "The silver bridge collapse recounted," *Journal of Performance of Constructed Facilities*, vol. 7, no. 4, pp. 249–261, 1993.

[8] U. Starossek, *Progressive Collapse of Structures*, Vol. 153, Thomas Telford Ltd., London, UK, 2009

[9] A.-A. Abolhassan, "Progressive collapse of steel truss bridges, the case of I-35W collapse," in *Proceedings of 7th International Conference on Steel Bridges*, Guimaraes, Portugal, June 2008.

[10] B. Kaiming, W.-X. Ren, P.-F. Cheng, and H. Ha, "Domino-type progressive collapse analysis of a multi-span simply-supported bridge: a case study," *Engineering Structures*, vol. 90, pp. 172–182, 2015.

[11] A. Ibarhim, H. Salim, and N. A. Rahman, "Progressive collapse of post-tensioned box girder bridges under blast loads using applied element method," in *Proceedings of 2012 Structures Congress*, pp. 2291–2300, Chicago, IL, USA, March 2012.

[12] Y. E. Lu and L. M. Zhang, "Progressive collapse of a drilled-shaft bridge foundation under vessel impact," *Ocean Engineering*, vol. 66, pp. 101–112, 2013.

[13] X. Zhen, X. Lu, H. Guan, X. Lu, and A. Ren, "Progressive-collapse simulation and critical region identification of a stone arch bridge," *Journal of Performance of Constructed Facilities*, vol. 27, no. 1, pp. 43–52, 2012.

[14] H. Salem and H. Helmy, "Numerical investigation of collapse of the Minnesota I-35W bridge," *Engineering Structures*, vol. 59, pp. 635–645, 2014.

[15] F. Seible, G. Hegemier, V. M. Karbhari, J. Wolfson, R. Conway, and J. D. Baum, "Protection of our bridge infrastructure against man-made and natural hazards," *Structure and Infrastructure Engineering*, vol. 4, no. 6, pp. 415–429, 2008.

[16] J. Guedes, "Seismic behavior of reinforced concrete bridges: modelling, numerical analysis, and experimental assessment," Ph.D. thesis, Department of Civil Engineering, University of Porto, Porto, Portugal, 1997.

[17] C. Chiara and P. Rui, "Seismic response of continuous span bridges through fiber-based finite element analysis," *Earthquake Engineering and Engineering Vibration*, vol. 5, no. 1, pp. 119–131, 2006.

[18] K. Meguro and T.-D. Hatem, "Applied element simulation for collapse analysis of structures," *Bulletin of Earthquake Resistant Structure Research Center*, vol. 32, pp. 113–123, 1999.

[19] H. Tagel-Din and K. Meguro, "Applied element method for dynamic large deformation analysis of structures," *Doboku Gakkai Ronbunshu*, vol. 661, pp. 1–10, 2000.

[20] H. Okamura and M. Kohichi, *Nonlinear Analysis and ConstitutiveModels of Reinforced Concrete*, Vol. 10, Gihodo, Tokyo, Japan, 1991.

[21] D. Ristic, "Stress-strain based modeling of hysteretic structures under earthquake induced bending and varying axial loads," Reseach Report No. 86-ST-01, School of Civil Engineering, Kyoto University, Kyoto, Japan, 1986.

[22] C. Cassarotti, R. Monteiro, and R. Pinho, "Verification of spectral reduction factors for seismic assessment of bridges," *Bulletin of the New Zealand Society for Earthquake Engineering*, vol. 42, no. 2, pp. 111–121, 2009.

[23] AASHTO, *Standard Specifications for Highway Bridges*,American Association of State Highway and Transportation Officials, Washington, DC, USA, 16th edition, 1997.

[24] U. Starossek, "Typology of progressive collapse," *Engineering Structures*, vol. 29, no. 9, pp. 2302–2307, 2007.

[25] ACI, *Building Code Requirements for Structural Concrete (ACI 318-05) and Commentary (ACI 318R-05)*, American Concrete Institute, Farmington Hills, MI, USA, 2005.

[26] Q. Han, X. Du, J. Liu, Z. Li, L. Li, and J. Zhao, "Seismic damage of highway bridges during the 2008 Wenchuan earthquake," *Earthquake Engineering and Engineering Vibration*, vol. 8, no. 2, pp. 263–273, 2009.

[27] A. Pamuk, E. Kalkan, and H.I. Ling, "Structural and geotechnical impacts of surface rupture on highway structures during recent earthquakes in Turkey," *Soil Dynamics and Earthquake Engineering*,vol. 25, no. 7, pp. 581–589, 2010.